Analysis of the Riemann Zeta Function via Recursive Taylor Expansions

Yunwei Bai (baiyunwei@u.nus.edu)

March 6, 2026

Abstract

We present an unconditional proof that non-trivial zeros of the Riemann Zeta function must lie strictly on the critical line $\mathrm{Re}(s) = 0.5$. By defining a recursive path of Taylor expansions originating from the domain of absolute convergence, we translate the zeta function towards the critical region, which is an easy-to-understand form of the analytical continuation. We then assume the existence of off-critical-line (off-line) zeros, which exist in pairs symmetric by the critical line. If the pairs are zero in value, their real and imaginary components differences should be both zero. However, we derive a contradiction against the assumption via basic logical deduction, proving the non-existence of the off-line zeros.

1 Introduction

The Riemann Hypothesis posits that all non-trivial zeros of the Zeta function $\zeta(s)$ have a real part equal to 1/2. While computational methods have verified this for trillions of zeros, a global analytic proof requires a mechanism to show that any deviation Δ from the critical line results in a non-vanishing value. This paper utilizes a recursive geometric approach to prove that the exact difference between symmetrically shifted coordinates off the critical line cannot collapse to zero.

Overall, we first derive a basic algebraic form of the analytical continuation via recursive taylor series expansion. Then, we assume that the off-line zeros exist. We define the paired zeros that are symmetric by the critical line as $p1$ and $p2$, and evaluate their real and imaginary differences, or RealDiff and ImagDiff for easy references, based on the analytical continuation. Though the differences are supposed to be both zero, basic logical deductions demonstrate the actual impossibility for the perfect balance of the zero, thus resulting in a contradiction and proving the hypothesis.

2 Preliminary: The Riemann's Hypothesis

Let $s = \sigma + it$ be a complex variable. The Riemann zeta function, $\zeta(s)$, is initially defined for $\mathrm{Re}(s) > 1$ by the absolutely convergent Dirichlet series:

$$\zeta(s) = \sum_{n=1}^{\infty} \frac{1}{n^s} \tag{2.1}$$

Through analytic continuation, $\zeta(s)$ extends to a meromorphic function on the entire complex plane $\mathbb{C}$, with its only singularity being a simple pole at $s = 1$. The extended function satisfies the Riemann functional equation:

$$\zeta(s) = 2^s \pi^{s-1} \sin\left(\frac{\pi s}{2}\right) \Gamma(1-s)\zeta(1-s) \tag{2.2}$$

where Γ denotes the gamma function.

From the functional equation, it follows that $\zeta(s)$ vanishes at the negative even integers ($s = -2, -4, -6, \dots$). These are known as the trivial zeros. All remaining zeros of $\zeta(s)$, known as the non-trivial zeros, are confined to the critical strip $0 \leq \mathrm{Re}(s) \leq 1$.
Conjecture (Riemann, 1859): All non-trivial zeros of the Riemann zeta function lie precisely on the critical line $\mathrm{Re}(s) = \frac{1}{2}$.
Formally, if $s \in \mathbb{C}$ is a zero of $\zeta(s)$ such that $0 \leq \mathrm{Re}(s) \leq 1$, then:

$$\mathrm{Re}(s) = \frac{1}{2} \tag{2.3}$$

3 Notation and Ordering Conventions

Indices. We work with multi–indices $\alpha = (\alpha_1, \alpha_2) \in \mathbb{N}_0^2$, $|\alpha| = \alpha_1 + \alpha_2$, $\alpha! = \alpha_1!\,\alpha_2!$, $(x-a)^\alpha = (x_1 - a_1)^{\alpha_1}(x_2 - a_2)^{\alpha_2}$. For $\beta, \alpha \in \mathbb{N}_0^2$, the partial order $\beta \geq \alpha$ means $\beta_k \geq \alpha_k$ for $k = 1, 2$ (componentwise).

Componentwise binomial. For $\beta \geq \alpha$,

$$\binom{\beta}{\alpha} := \binom{\beta_1}{\alpha_1}\binom{\beta_2}{\alpha_2}, \qquad (\beta - \alpha)! := (\beta_1 - \alpha_1)!\,(\beta_2 - \alpha_2)!.$$

4 The Chained Disk Formulation

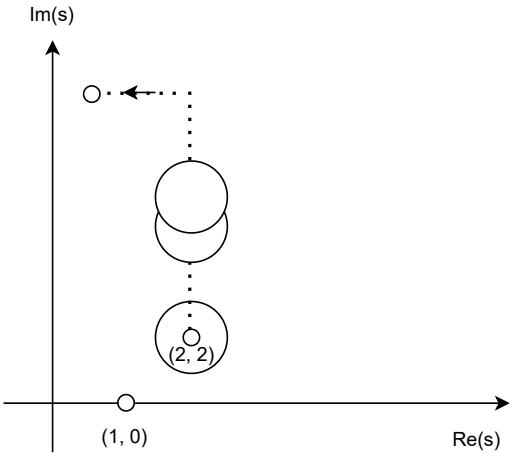

Figure 1: We start from the location (2, 2) in the complex plane and taylor expand the zeta function to obtain a disk of radius 0.5 that does not touch the pole. We then always shift the base disk upward by 0.5 in distance, before finally shifting the disk leftward by three 0.5-distance steps and then a step less than or equal to 0.5, and the final vertical shift can be an arbitrary value less than or equal to 0.5 as well. All the disks are chained via overlapping points; the top tip of the previous disk becomes the center of the new disk. By starting at (2, 2) and constraining the disk radius to 0.5, we avoid the pole at (1, 0). Through the recursive formulation, we derive an alternative form of analytical continuation that covers the entire upper part above Im(s)= 2 of the critical strip. Note that all graphs are non-exact in details and only serve the illustration purpose.

To avoid the singularity at $s = 1$ while shifting towards the critical line, we adjust the starting location and the path geometry. An overview illustration is available in Figure 1.

4.1 Starting Point

We set the starting point to:

$$a_0 = 2 + 2i \tag{4.1}$$

4.2 Path Steps

The path consists of t steps defined as follows:

1. **Vertical Shifts:** The vertical shifts are constant at 0.5 for all steps except the final one.

$$\Delta_{g2} = 0.5 \quad (g = 1, \ldots, t-1) \tag{4.2}$$
$$\Delta_{t,2} = v2 \quad \text{(Final Step, where } v2 \in [0, 0.5]) \tag{4.3}$$

2. **Horizontal Shifts:** We utilize 3 standard steps of length 0.5 to the left to reach the critical region, followed by the final symmetric difference shift.

$$\Delta_{g1} = -0.5 \quad (g = t-1, t-2, t-3) \tag{4.4}$$
$$\Delta_{t,1} = v1 \quad \text{(Final Step, where } v1 \in [0, 0.5]) \tag{4.5}$$

Definition 4.1 (Coefficients at stage g)**.** Fix $g \geq 1$. Let $a_{g-1}, a_g \in \mathbb{C} \setminus \{1\}$. Assume coefficients $R(g-1;\beta)$ are defined for all $\beta \in \mathbb{N}_0^2$. Let $\Delta_g = a_g - a_{g-1}$. For $\alpha \in \mathbb{N}_0^2$ define

$$R(g;\alpha) := \sum_{\beta \geq \alpha} \frac{\Delta_g^{\beta-\alpha}}{(\beta-\alpha)!} R(g-1;\beta) \tag{4.6}$$

4.3 Base Derivatives at $a_0 = 2 + 2i$

We compute the derivatives of the Dirichlet series at $a_0 = 2 + 2i$. The mixed partial derivative term is:

$$\partial^{(\theta_1^0,\theta_2^0)}\zeta(a_0) = \sum_{n=1}^{\infty} (-1)^{\theta_1^0} (\ln n)^{\theta_1^0} n^{-(2+2i)} (-i)^{\theta_2^0} (\ln n)^{\theta_2^0} \tag{4.7}$$
$$= (-1)^{\theta_1^0} (-i)^{\theta_2^0} \sum_{n=1}^{\infty} n^{-2} (\ln n)^{\theta_1^0+\theta_2^0} e^{-i2\ln n} \tag{4.8}$$

For the real part of this expression, we recall $(-i)^{\theta_2^0} = e^{-i\frac{\pi}{2}\theta_2^0}$.

$$\Re[\ldots] = (-1)^{\theta_1^0} \sum_{n=1}^{\infty} n^{-2} (\ln n)^{\theta_1^0+\theta_2^0} \Re\left[e^{-i(\frac{\pi}{2}\theta_2^0 + 2\ln n)}\right] \tag{4.9}$$
$$= (-1)^{\theta_1^0} \sum_{n=1}^{\infty} n^{-2} (\ln n)^{\theta_1^0+\theta_2^0} \cos\left(\frac{\pi}{2}\theta_2^0 + 2\ln n\right). \tag{4.10}$$

For the imaginary part, we have:

$$\Im[\ldots] = (-1)^{\theta_1^0} \sum_{n=1}^{\infty} n^{-2} (\ln n)^{\theta_1^0+\theta_2^0} \Im\left[e^{-i(\frac{\pi}{2}\theta_2^0 + 2\ln n)}\right] \tag{4.11}$$
$$= (-1)^{\theta_1^0} \sum_{n=1}^{\infty} n^{-2} (\ln n)^{\theta_1^0+\theta_2^0} \left(-\sin\left(\frac{\pi}{2}\theta_2^0 + 2\ln n\right)\right). \tag{4.12}$$

4.4 Recursive Zeta Function Representation

To decouple the analytical continuation into explicit real and imaginary formulations for the subsequent derivation of RealDiff and ImagDiff, we separate the complex coefficients $R(g;\alpha)$ in Eqn 4.6 into their real part $U(g;\alpha) = \Re[R(g;\alpha)]$ and imaginary part $V(g;\alpha) = \Im[R(g;\alpha)]$.

Given that the step difference $\Delta_g = (\Delta_{g,1}, \Delta_{g,2})$ represents purely real spatial shifts along the real and imaginary axes, the multi-index term $\Delta_g^{\beta-\alpha}$ expands strictly as a real-valued multiplier: $\Delta_{g,1}^{\beta_1-\alpha_1}\Delta_{g,2}^{\beta_2-\alpha_2}$.

Thus, the explicit single-step recursive representations for the Real and Imaginary components are defined as:

$$U(g;\theta^g) = \sum_{\theta^{g-1}\geq\theta^g} \frac{\Delta_{g,1}^{\theta_1^{g-1}-\theta_1^g}\Delta_{g,2}^{\theta_2^{g-1}-\theta_2^g}}{(\theta_1^{g-1}-\theta_1^g)!(\theta_2^{g-1}-\theta_2^g)!}U(g-1;\theta^{g-1})$$

$$V(g;\theta^g) = \sum_{\theta^{g-1}\geq\theta^g} \frac{\Delta_{g,1}^{\theta_1^{g-1}-\theta_1^g}\Delta_{g,2}^{\theta_2^{g-1}-\theta_2^g}}{(\theta_1^{g-1}-\theta_1^g)!(\theta_2^{g-1}-\theta_2^g)!}V(g-1;\theta^{g-1})$$

where we have adopted the notation $\theta^g = (\theta_1^g, \theta_2^g)$ to represent the multi-index at stage g, setting up the sequence of indices $\theta^0, \theta^1, \ldots, \theta^t$ as we trace back to the base derivative at $a_0 = 2 + 2i$.

To obtain the full chain-disk algebraic representation from stage t down to the base a_0 (where $g = 0$), we recursively expand the above single-step formulas. By substituting $U(g-1;\theta^{g-1})$ with its own expansion, and repeating this process down to $U(0;\theta^0)$, we accumulate a nested summation over all intermediate multi-indices:

$$U(t;\theta^t) = \sum_{\theta^{t-1}\geq\theta^t}\sum_{\theta^{t-2}\geq\theta^{t-1}}\cdots\sum_{\theta^0\geq\theta^1}\left[\prod_{g=1}^{t}\frac{\Delta_{g,1}^{\theta_1^{g-1}-\theta_1^g}}{(\theta_1^{g-1}-\theta_1^g)!}\frac{\Delta_{g,2}^{\theta_2^{g-1}-\theta_2^g}}{(\theta_2^{g-1}-\theta_2^g)!}\right]U(0;\theta^0)$$

$$V(t;\theta^t) = \sum_{\theta^{t-1}\geq\theta^t}\sum_{\theta^{t-2}\geq\theta^{t-1}}\cdots\sum_{\theta^0\geq\theta^1}\left[\prod_{g=1}^{t}\frac{\Delta_{g,1}^{\theta_1^{g-1}-\theta_1^g}}{(\theta_1^{g-1}-\theta_1^g)!}\frac{\Delta_{g,2}^{\theta_2^{g-1}-\theta_2^g}}{(\theta_2^{g-1}-\theta_2^g)!}\right]V(0;\theta^0)$$

These unrolled equations explicitly link the coefficients at the final targeted evaluation point t to the base derivatives. The real base term $U(0;\theta^0)$ corresponds to the real part of the mixed partial derivatives of $\zeta(s)$ at a_0 , and $V(0;\theta^0)$ corresponds to the imaginary part:

$$U(0;\theta^0) = (-1)^{\theta_1^0}\sum_{n=1}^{\infty} n^{-2}(\ln n)^{\theta_1^0+\theta_2^0}\cos\left(\frac{\pi}{2}\theta_2^0 + 2\ln n\right) \tag{4.13}$$

$$V(0;\theta^0) = (-1)^{\theta_1^0}\sum_{n=1}^{\infty} n^{-2}(\ln n)^{\theta_1^0+\theta_2^0}\left(-\sin\left(\frac{\pi}{2}\theta_2^0 + 2\ln n\right)\right) \tag{4.14}$$

Because the geometric path shifts ($\Delta_{g,1}$ and $\Delta_{g,2}$) are strictly real, the separation of real and imaginary components established at the base is perfectly preserved through the entire recursive chain. More detailed derivations of the recursive real or imaginary representation are available in Appendix Section A.

5 Derivation of RealDiff and ImagDiff

5.1 Definitions of Exact Differences

To prove the Riemann Hypothesis, we evaluate whether two symmetric points p1 and p2 shifted off the critical line, as illustrated by Figure 2, can equal 0 in difference. We explicitly define RealDiff

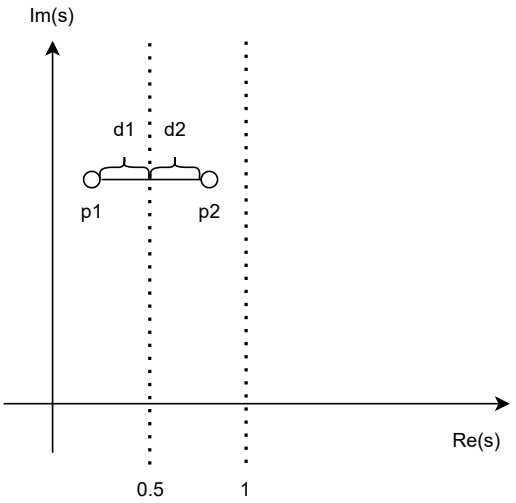

Figure 2: Two symmetric points p1 and p2 shifted off the critical line by the same horizontal distance (i.e., d1 = d2). Their real/imaginary differences are evaluated.

and ImagDiff as the exact geometric sums that compute the difference in the real and imaginary components between evaluating the sequence at $0.5 + \Delta_{t,1} + i\text{Im(s)}$ and $0.5 - \Delta_{t,1} + i\text{Im(s)}$.

5.2 Updated RealDiff Formula

We assemble the components: *1.* Horizontal Path: Common path (steps $1..t-1$) with $\Delta = 0$ or $\Delta = -0.5$, and final jump $\Delta_{t,1}$. *2.* Vertical Path: Steps $1..t-1$ with $\Delta = 0.5$, and final jump $\Delta_{t,2}$. *3.* Base Term: The phase-shifted cosine/sine term derived above.

$$
\begin{aligned}
\text{RealDiff} = & \sum_{\theta_1^0 \geq \ldots \geq \theta_1^{t-1} \geq 0} \quad \sum_{\theta_2^0 \geq \cdots \geq \theta_2^{t-2} \geq 0} \\
& \underbrace{\left[\prod_{g=1}^{t-4} \frac{(0)^{\theta_1^{g-1} - \theta_1^g}}{(\theta_1^{g-1} - \theta_1^g)!} \right]}_{\text{Inactive Horiz. Steps}} \times \underbrace{\left[\prod_{g=t-3}^{t-1} \frac{(-0.5)^{\theta_1^{g-1} - \theta_1^g}}{(\theta_1^{g-1} - \theta_1^g)!} \right]}_{\text{Inactive Horiz. Steps } (t-3 \ldots t-1)} \times \underbrace{\left[\frac{(\Delta_{t,1})^{\theta_1^{t-1}}}{(\theta_1^{t-1})!} - \frac{(-\Delta_{t,1})^{\theta_1^{t-1}}}{(\theta_1^{t-1})!} \right]}_{\text{Final Horizontal Jump}} \times \\
& \underbrace{\left[\frac{(\Delta_{t,2})^{\theta_2^{t-1}}}{(\theta_2^{t-1})!} \right]}_{\text{Final Vertical Jump}} \times \underbrace{\left[\prod_{g=1}^{t-1} \frac{(0.5)^{\theta_2^{g-1} - \theta_2^g}}{(\theta_2^{g-1} - \theta_2^g)!} \right]}_{\text{Full Vertical Path}} \\
& \times \underbrace{(-1)^{\theta_1^0}}_{\text{Sign}} \underbrace{\sum_{n=1}^{\infty} n^{-2} (\ln n)^{\theta_1^0 + \theta_2^0} \cos\left(\frac{\pi}{2} \theta_2^0 + 2 \ln n \right)}_{\text{Base Term}} \\
= & \, 2 \times 1 \times \sum_{\substack{\theta_1^0 = \theta_1^{t-4} \geq \ldots \geq \theta_1^{t-1} \geq 1 \\ \theta_1^{t-1} \equiv 1 \pmod 2}} \quad \sum_{\theta_2^0 \geq \cdots \geq \theta_2^{t-2} \geq 0} \\
& \underbrace{\left[\prod_{g=t-3}^{t-1} \frac{(-0.5)^{\theta_1^{g-1} - \theta_1^g}}{(\theta_1^{g-1} - \theta_1^g)!} \right]}_{\text{Active Horiz. Steps } (t-3 \ldots t-1)} \times \underbrace{\left[\frac{(\Delta_{t,1})^{\theta_1^{t-1}}}{(\theta_1^{t-1})!} \right]}_{\text{Final Horizontal Jump}} \times \underbrace{\left[\frac{(\Delta_{t,2})^{\theta_2^{t-1}}}{(\theta_2^{t-1})!} \right]}_{\text{Final Vertical Jump}} \times \underbrace{\left[\prod_{g=1}^{t-1} \frac{(0.5)^{\theta_2^{g-1} - \theta_2^g}}{(\theta_2^{g-1} - \theta_2^g)!} \right]}_{\text{Full Vertical Path}} \\
& \times \underbrace{(-1)^{\theta_1^0}}_{\text{Sign}} \underbrace{\sum_{n=1}^{\infty} n^{-2} (\ln n)^{\theta_1^0 + \theta_2^0} \cos\left(\frac{\pi}{2} \theta_2^0 + 2 \ln n \right)}_{\text{Base Term}}
\end{aligned}
\tag{5.1}
$$

5.3 Derivation of ImagDiff

Using the identical horizontal and vertical path geometries defined for RealDiff, the final ImagDiff equation is:

$$
\begin{aligned}
\text{ImagDiff} = 2 & \sum_{\substack{\theta_1^0 = \theta_1^{t-4} \geq \cdots \geq 1 \\ \theta_1^{t-1} \equiv 1 \pmod 2}} \quad \sum_{\theta_2^0 \geq \cdots \geq 0} \\
& \underbrace{\left[\prod_{g=t-3}^{t-1} \frac{(-0.5)^{\theta_1^{g-1} - \theta_1^g}}{(\theta_1^{g-1} - \theta_1^g)!} \right]}_{\text{Active Horiz. Steps}} \times \underbrace{\left[\frac{(\Delta_{t,1})^{\theta_1^{t-1}}}{(\theta_1^{t-1})!} \right]}_{\text{Final Horizontal Jump}} \times \\
& \underbrace{\left[\frac{(\Delta_{t,2})^{\theta_2^{t-1}}}{(\theta_2^{t-1})!} \right]}_{\text{Final Vertical Jump}} \times \underbrace{\left[\prod_{g=1}^{t-1} \frac{(0.5)^{\theta_2^{g-1} - \theta_2^g}}{(\theta_2^{g-1} - \theta_2^g)!} \right]}_{\text{Full Vertical Path}} \\
& \times (-1)^{\theta_1^0} \sum_{n=1}^{\infty} n^{-2} (\ln n)^{\theta_1^0 + \theta_2^0} \left(-\sin\left(\frac{\pi}{2} \theta_2^0 + 2 \ln n \right) \right)
\end{aligned}
\tag{5.2}
$$

5.4 RealDiff and ImagDiff Simplification

We are not interested in evaluating the RealDiff and ImagDiff exact values, and aggregate constant factors into a combined factor C. Focusing on the formula 5.1, any terms not related to the indices $\theta_1^0 = \theta_1^{t-4}$ and θ_2^0 evaluate to constants, as the terms are always decreasing with $0 \leq \Delta \leq 0.5$, and

their indices ranges do not affect the base term (e.g., $\sum_{a\in[0,\infty],b\in[0,\infty]} A_a B_b = \sum_{a\in[0,\infty]} A_a \sum_{b\in[0,\infty]} B_b$). Besides, the sign term $(-1)^{\theta_1^0}$ is also a constant factor to be merged into C, as it is not affected by θ_2^0. In our analysis later, we fix θ_1^0 and all other variables except θ_2^0. Therefore, any constant factors not affected by θ_2^0 can be simplified (See later sections). Overall, we have:

$$\begin{aligned}\text{RealDiff} = 2 \sum_{\theta_1^{t-4}\geq 1} \sum_{\theta_2^0\geq 0} C \cdot \frac{(0.5)^{\theta_1^{t-4}}}{(\theta_1^{t-4})!} \frac{(0.5)^{\theta_2^0}}{(\theta_2^0)!} \times \\ \times \sum_{n=1}^{\infty} n^{-2} (\ln n)^{\theta_1^{t-4}+\theta_2^0} \cos\left(\frac{\pi}{2}\theta_2^0 + 2\ln n\right),\end{aligned} \tag{5.3}$$

$$\begin{aligned}-\text{ImagDiff} = 2 \sum_{\theta_1^{t-4}\geq 1} \sum_{\theta_2^0\geq 0} C \cdot \frac{(0.5)^{\theta_1^{t-4}}}{(\theta_1^{t-4})!} \frac{(0.5)^{\theta_2^0}}{(\theta_2^0)!} \\ \times \sum_{n=1}^{\infty} n^{-2} (\ln n)^{\theta_1^{t-4}+\theta_2^0} \sin\left(\frac{\pi}{2}\theta_2^0 + 2\ln n\right),\end{aligned} \tag{5.4}$$

and

$$\begin{aligned}\text{RealDiff} - i\text{ImagDiff} = 2 \sum_{\theta_1^{t-4}\geq 1} \sum_{\theta_2^0\geq 0} C \cdot \frac{(0.5)^{\theta_1^{t-4}}}{(\theta_1^{t-4})!} \frac{(0.5)^{\theta_2^0}}{(\theta_2^0)!} \\ \times \sum_{n=1}^{\infty} n^{-2} (\ln n)^{\theta_1^{t-4}+\theta_2^0} \\ \times \left[\cos\left(\frac{\pi}{2}\theta_2^0 + 2\ln n\right) + i\sin\left(\frac{\pi}{2}\theta_2^0 + 2\ln n\right)\right].\end{aligned} \tag{5.5}$$

5.5 Trigonometric Expansion and Structural Alignment

We apply the trigonometric addition formulas to the complex exponential components:

$$\cos\left(\frac{\pi}{2}\theta_2^0 + 2\ln n\right) = \cos\left(\frac{\pi}{2}\theta_2^0\right)\cos(2\ln n) - \sin\left(\frac{\pi}{2}\theta_2^0\right)\sin(2\ln n) \tag{5.6}$$

$$\sin\left(\frac{\pi}{2}\theta_2^0 + 2\ln n\right) = \sin\left(\frac{\pi}{2}\theta_2^0\right)\cos(2\ln n) + \cos\left(\frac{\pi}{2}\theta_2^0\right)\sin(2\ln n) \tag{5.7}$$

Substituting these expansions into the equation 5.5, we obtain:

$$\begin{aligned}\text{RealDiff} - i\text{ImagDiff} &= 2 \sum_{\theta_1^{t-4}\geq 1} \sum_{\theta_2^0\geq 0} C \cdot \frac{(0.5)^{\theta_1^{t-4}}}{\theta_1^{t-4}!} \frac{(0.5)^{\theta_2^0}}{\theta_2^0!} \sum_{n=1}^{\infty} n^{-2} (\ln n)^{\theta_1^{t-4}+\theta_2^0} \\ &\quad \times \Bigg[\Big(\cos\left(\frac{\pi}{2}\theta_2^0\right)\cos(2\ln n) - \sin\left(\frac{\pi}{2}\theta_2^0\right)\sin(2\ln n)\Big) \\ &\quad + i\Big(\sin\left(\frac{\pi}{2}\theta_2^0\right)\cos(2\ln n) + \cos\left(\frac{\pi}{2}\theta_2^0\right)\sin(2\ln n)\Big)\Bigg] \\ &= \sum_{\theta_1^{t-4}\geq 1} \sum_{\theta_2^0\geq 0} C \cdot \frac{(0.5)^{\theta_1^{t-4}}}{\theta_1^{t-4}!} \frac{(0.5)^{\theta_2^0}}{\theta_2^0!} \sum_{n=1}^{\infty} n^{-2} (\ln n)^{\theta_1^{t-4}+\theta_2^0} \\ &\quad \times \Bigg[\underbrace{\Big(\cos\left(\frac{\pi}{2}\theta_2^0\right)\cos(2\ln n) + \sin\left(\frac{\pi}{2}\theta_2^0\right)\cos(2\ln n)\cdot i\Big)}_{\text{Term 1}} + \\ &\quad \underbrace{\Big(-\sin\left(\frac{\pi}{2}\theta_2^0\right)\sin(2\ln n) + \cos\left(\frac{\pi}{2}\theta_2^0\right)\sin(2\ln n)\cdot i\Big)}_{\text{Term 2}}\Bigg]\end{aligned} \tag{5.8}$$

Because the index $\theta_2^0 \in \mathbb{N}_0$ is strictly an integer, the base trigonometric functions evaluating $\frac{\pi}{2}\theta_2^0$ are mutually exclusive. We factor the remaining terms associated with Term 1:

$$
\begin{aligned}
(\text{RealDiff} - i\text{ImagDiff})_{\text{Term 1}} = & \sum_{\theta_1^{t-4} \geq 1} \\
& \Bigg(\sum_{\theta_2^0 \equiv 0 \pmod 4} \sum_{n=1}^{\infty} C \frac{(0.5)^{\theta_1^{t-4}} (0.5)^{\theta_2^0}}{\theta_1^{t-4}! \theta_2^0!} n^{-2} (\ln n)^{\theta_1^{t-4} + \theta_2^0} \\
& - \sum_{\theta_2^0 \equiv 2 \pmod 4} \sum_{n=1}^{\infty} C \frac{(0.5)^{\theta_1^{t-4}} (0.5)^{\theta_2^0}}{\theta_1^{t-4}! \theta_2^0!} n^{-2} (\ln n)^{\theta_1^{t-4} + \theta_2^0} \\
& + i \sum_{\theta_2^0 \equiv 1 \pmod 4} \sum_{n=1}^{\infty} C \frac{(0.5)^{\theta_1^{t-4}} (0.5)^{\theta_2^0}}{\theta_1^{t-4}! \theta_2^0!} n^{-2} (\ln n)^{\theta_1^{t-4} + \theta_2^0} \\
& - i \sum_{\theta_2^0 \equiv 3 \pmod 4} \sum_{n=1}^{\infty} C \frac{(0.5)^{\theta_1^{t-4}} (0.5)^{\theta_2^0}}{\theta_1^{t-4}! \theta_2^0!} n^{-2} (\ln n)^{\theta_1^{t-4} + \theta_2^0} \Bigg) \\
& \times \cos(2 \ln n).
\end{aligned} \tag{5.9}
$$

For Term 2, we have:

$$
\begin{aligned}
(\text{RealDiff} - i\text{ImagDiff})_{\text{Term 2}} = & \sum_{\theta_1^{t-4} \geq 1} \\
& \Bigg(i \sum_{\theta_2^0 \equiv 0 \pmod 4} \sum_{n=1}^{\infty} C \frac{(0.5)^{\theta_1^{t-4}} (0.5)^{\theta_2^0}}{\theta_1^{t-4}! \theta_2^0!} n^{-2} (\ln n)^{\theta_1^{t-4} + \theta_2^0} \\
& - \sum_{\theta_2^0 \equiv 1 \pmod 4} \sum_{n=1}^{\infty} C \frac{(0.5)^{\theta_1^{t-4}} (0.5)^{\theta_2^0}}{\theta_1^{t-4}! \theta_2^0!} n^{-2} (\ln n)^{\theta_1^{t-4} + \theta_2^0} \\
& - i \sum_{\theta_2^0 \equiv 2 \pmod 4} \sum_{n=1}^{\infty} C \frac{(0.5)^{\theta_1^{t-4}} (0.5)^{\theta_2^0}}{\theta_1^{t-4}! \theta_2^0!} n^{-2} (\ln n)^{\theta_1^{t-4} + \theta_2^0} \\
& + \sum_{\theta_2^0 \equiv 3 \pmod 4} \sum_{n=1}^{\infty} C \frac{(0.5)^{\theta_1^{t-4}} (0.5)^{\theta_2^0}}{\theta_1^{t-4}! \theta_2^0!} n^{-2} (\ln n)^{\theta_1^{t-4} + \theta_2^0} \Bigg) \\
& \times \sin(2 \ln n).
\end{aligned} \tag{5.10}
$$

Note that $\cos(0 \cdot \pi/2) = 1$, $\cos(2 \cdot \pi/2) = -1$, $\sin(\pi/2) = 1$ and $\sin(3 \cdot \pi/2) = -1$. Also, $\text{RealDiff} - i\text{ImagDiff} = (\text{RealDiff} - i\text{ImagDiff})_{\text{Term 1}} + (\text{RealDiff} - i\text{ImagDiff})_{\text{Term 2}}$.

In the following sections, based on the derived representation, we show that it is impossible for RealDiff - ImagDiff$\cdot i$ to equal zero, and thus the non-trivial 0s do not exist on the critical line. Appendices include why we can consider the difference; we first explain why that RealDiff - ImagDiff$\cdot i = 0$ is a necessary condition for the existence of off-line non-trivial zeros in Appendix Section B, and then we prove why covering only the upper part of the critical strip simultaneously covers the analysis for the lower part of the critical strip in Appendix Section C.

6 Term 1 Realness Imbalance

To make the 5.8 zero, we can 1) make the sum associated with the Term 1 zero while making the sum associated with Term 2 zero (e.g., $\sum$ Term-1-Related-Real + $\sum$ Term-1-Related-Imag = 0); alternatively, we can 2) make the sum associated with both Term 1 and Term 2 zero (e.g., $\sum$ Term-1-Real + $\sum$ Term-1-Imag $\neq$ 0 and $\sum$ Term-1-Real + $\sum$ Term-1-Imag + $\sum$ Term-2-Real + $\sum$ Term-2-Imag = 0). We analyse the case

1 (single-term) possibility in this section, and the case 2 (cross-term) and overall balance possibility in Section 7. For case 1 to be proved as impossible, we can just focus on the zero impossibility of either the Term 1 related components, or the Term 2 related terms, instead of both the Term 1 and 2. This is because either term's balance is the necessary condition for case 1. We now focus on the Term 1. Our goal is to prove the single-term balance impossibility within the Term 1 related components.

6.1 Graph Set-up

We first focus on the **Term 1** and refer to the following expression as the "Base Component":

$$\frac{(0.5)^{\theta_1^{t-4}}(0.5)^{\theta_2^0}}{\theta_1^{t-4}!\theta_2^0!}n^{-2}(\ln n)^{\theta_1^{t-4}+\theta_2^0} = \left[\frac{(0.5)^k}{k!}n^{-2}(\ln n)^k\right]\cdot\frac{(0.5\ln n)^x}{x!}, \tag{6.1}$$

where $x = \theta_2^0$ and let $k = \theta_1^{t-4}$. We assume RealDiff - ImagDiff$\cdot i = 0$ and first convert the (RealDiff - ImagDiff$\cdot i)_{\text{Term 1}}$ expression to graph representations. We fix n and θ_1^{t-4} to any general valid value. Note that the same constant factor C is shared across indices $\theta_2^0\%4 \in \{0,1,2,3\}$ of the base component, as the θ_2^0 does not affect C and we fix all the remaining variables that contribute to C.

We plot each base component on a plane, where the y-axis denotes the absolute real-valued base component magnitude, and the x-axis denotes the real-valued θ_2^0 value. We call the graph type "absolute graph" as it denotes the absolute magnitudes of the base component associated with each index θ_2^0.

Obviously, being a continuous, smooth and positive-valued expression that decreases and approaches an asymptote at the end (e.g., in the form of $\frac{0.5^\theta}{\theta!}(\ln n)^\theta$, where the $(\ln n)$ term always changes slower than the $\frac{0.5^\theta}{\theta!}$ term near the end), when θ_2^0 approaches infinity, the absolute base formula **must** belong to one of the following types:

1. Type A: an "empty" graph where the base formula evaluates to 0 (i.e., when n equals 1).
2. Type B: a positive, decreasing curve. This type does not have a "turning point peak", and happens only when n equals 2.
3. Type C: a positive curve that initially increases until a peak turning point (TP), and then decreases. Before the TP, the curve is purely concave.
4. Type D: a positive, bell-shaped curve that initially increases until a peak turning point (TP), and then decreases. Before the TP, the curve is first convex and then concave.

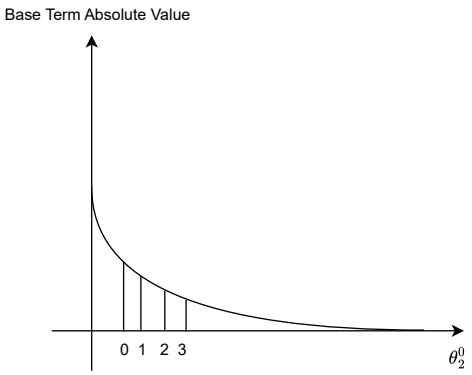

Figure 3: Type B absolute graph, a positive, decreasing curve.

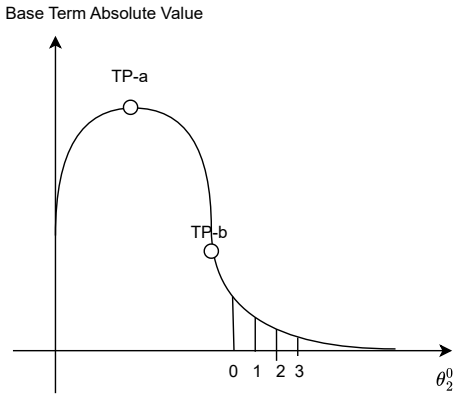

Figure 4: Type C absolute graph, a positive curve that initially increases until a peak turning point TP-a, and then decreases, in which there is an inflection point TP-b.

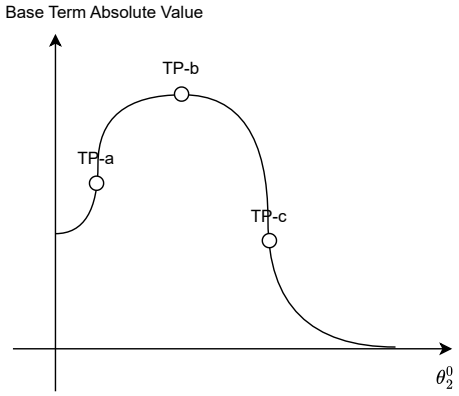

Figure 5: Type D absolute graph. Same as Type C except the existence of the inflection point TP-a.

We ignore Type A because it does not make any difference. Figures 3, 4 and 5 illustrate the B, C and D graph types respectively.

Next, we analyse the positive/negative or real/imaginary components based on the graphs, where we **assume perfect positivity balance** throughout and **analyse the realness balance**. Note that the B/C/D graphs are formed by base component values evaluated at an infinite amount of $\theta_2^0 \% 4 \in \{0, 1, 2, 3\}$ groups, each looping sequentially within the index set. We denote each of the base component value magnitude evaluated at $\theta_2^0 \% 4$ as h_0, h_1, h_2 or h_3. Here, we assume that the turning points of all base component graphs happen exactly at the last index 3, so that the grouping is exact. We will cover the other cases (i.e., at index 0, 1 or 2) in Section 6.7.

For each of the 3 original absolute graphs, we plot two other types of graph. The first graph is a plane where the y-axis positive direction denotes the actual positive magnitude of the (non-absolute) value of the base component, associated with each full index group (i.e., $\theta_2^0 \in \{0, 1, 2, 3\}$). The negative direction denotes the actual negative magnitude of the base component. We call the graph the "positivity graph", as it denotes if the base component expression is positive or negative at different θ_2^0 group indices. The second graph is a plane where the y-axis positive direction denotes the real-value magnitude of the base component associated with each full index group, and the y-axis negative direction denotes the imaginary-value magnitude. We call the graph the "realness graph", as it denotes if the base component expression is real or imaginary at different θ_2^0 group indices.

Additionally, to recap, each index type $\theta_2^0 \% 4$ contributes to the (RealDiff - ImagDiff$\cdot i)_{\text{Term 1}}$ in the following manner (See Eqn 5.9):

1. Positive component: Indices 0, 1
2. Negative component: Indices 2, 3
3. Real Component: Indices 0, 2
4. Imaginary Component: Indices 1, 3

6.2 Type B Graph

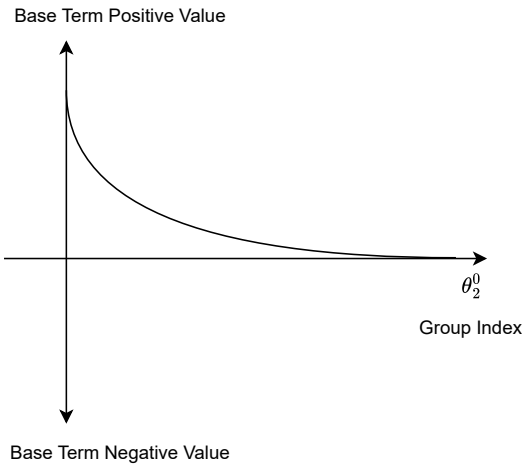

Figure 6: Type B positivity graph.

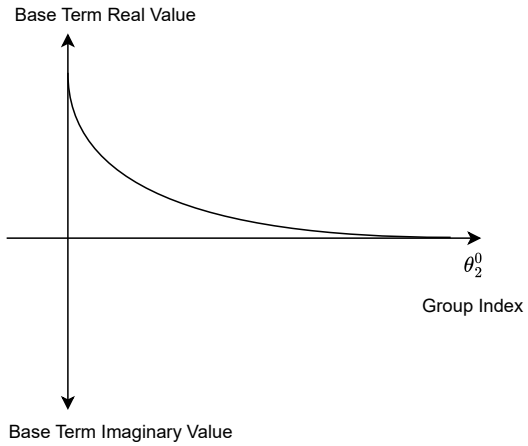

Figure 7: Type B realness graph, which is always real and smaller than the positivity graph in area size.

We first evaluate the type B absolute graph in Figure 3, which can be converted to the Figure 6 positivity graph and the Figure 7 realness graph.

Note that in the positivity graph, all values are positive. This is because any index group in the absolute graph follows the pattern: $h_0 > h_1 > h_2 > h_3$. Recall that indices 0 and 1 contribute to the positive component. Therefore, each group brings about $h_0 + h_1 - (h_2 + h_3) > 0$ magnitude in the positive direction.

In the realness graph, all values are real. Recall that indices 0 and 2 contribute to the real component and $h_0 > h_1 > h_2 > h_3$. Therefore, $h_0 + h_2 > h_1 + h_3$, where each group brings about $h_0 + h_2 - (h_1 + h_3) > 0$ magnitude in the real direction.

Besides, we notice that the Type B realness graph (made up from magnitudes of $h_0+h_2-(h_1+h_3)$) is always real and smaller than the positivity graph (made up from magnitudes of $h_0+h_1-(h_2+h_3)$) in area size, because $h_0+h_2-(h_1+h_3)-(h_0+h_1-(h_2+h_3)) = 2(h2-h1) < 0$. The different-index components share the exact same format across the positivity and realness component formula (See 5.9). Therefore, in Type B, compared to the positive magnitude, the real magnitude always falls short by the $2|h_2 - h_1|$ units.

6.3 Type C Graph

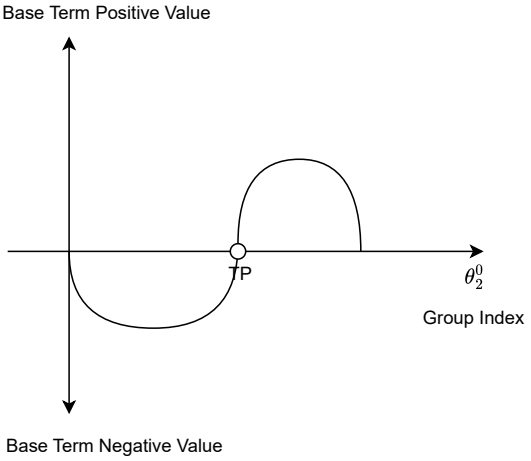

Figure 8: Type C positivity graph.

We next evaluate the type C absolute graph in Figure 3, which can be converted to the Figure 8 positivity graph and the Figure 9 realness graph.

In the positivity graph, all values to the left of the peak turning point TP are negative, whose area is equivalent to the sum across different θ_2^0 group indices, and becomes positive to the right of the peak turning point. Any index group in the absolute graph follows the pattern: $h_0 < h_1 < h_2 < h_3$ before reaching the peak turning point, and follows the pattern $h_0 > h_1 > h_2 > h_3$ after reaching the peak turning point. In the realness graph, all values are imaginary to the left of the peak turning point, and becomes real to the right of the peak turning point, by the same reasoning.

It is obvious that the turning points of the positivity graph and the realness graph are the same turning point corresponding to the single turning point of the original absolute graph. Besides, recall that indices 0 and 1 contribute to positivity, and indices 0 and 2 contribute to realness. To the left of the turning point, the imaginary region is made up from magnitudes of $h_1+h_3-(h_0+h_2) > 0$. Then, we compare the positive-imaginary difference: $h_2+h_3-(h_0+h_1)-(h_1+h_3-(h_0+h_2)) = 2(h_2-h_1) > 0$. In other words, to the left of the turning point, the imaginary region is smaller than the negative region.

To the right of the turning point, the positive region is made up from vertical lines of the magnitude $h_0 + h_1 - (h_2 + h_3) > 0$, while the real region is made up from $h_0 + h_2 - (h_1 + h_3) > 0$. Since

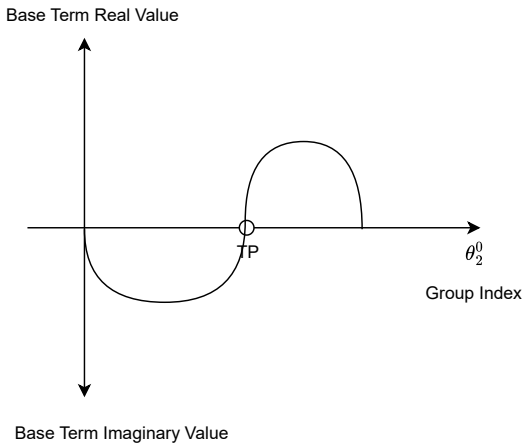

Figure 9: Type C realness graph. The two regions are separated to the left and right of the turning point TP. If we treat the positivity graph area balance as the groundtruth, the relative realness strength falls short.

$h_0 > h_1 > h_2 > h_3$ after TP, we have, for each index group real and positivity difference: $h_0 + h_2 - (h_1 + h_3) - (h_0 + h_1 - (h_2 + h_3)) = 2(h2 - h1) < 0$. In other words, to the right of the turning point, the real region is smaller than the positive region.

Overall, we have the cumulative difference of $2|h_2 - h_1|$ on both the left and right sides, and the two realness regions are smaller than the corresponding positivity regions. We will analyse the realness balance after we cover the Type D graph.

6.4 Type D Graph

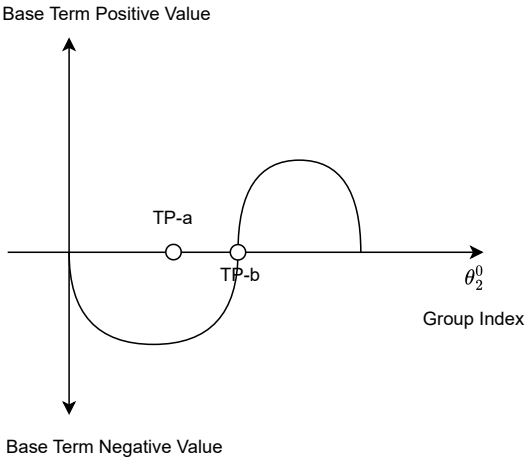

Figure 10: Type D positivity graph.

We next evaluate the Type D absolute graph in Figure 5, which can be converted to the Figure 8 positivity graph and the Figure 9 realness graph.

For the positivity and realness graph, overall shapes are the same as those in Type C. Recall that

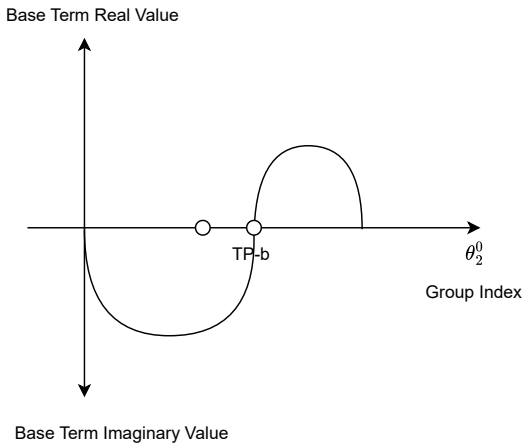

Figure 11: Type D realness graph. If we treat the positivity graph area balance as the groundtruth, the relative realness strength falls short.

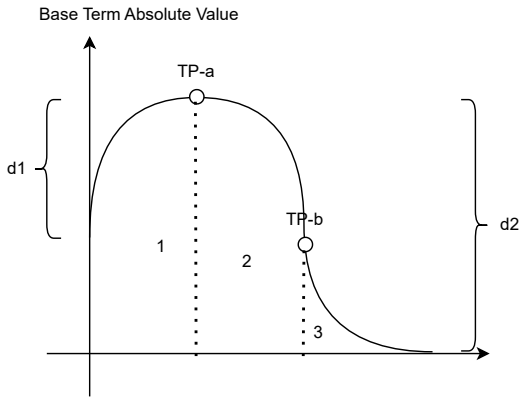

Figure 12: Type C graph characteristics. Depth d_1 is larger in magnitude compared to d_2. Region 2 + Region 3 > Region 1.

indices 0, 1 contribute to the positive terms, and the indices 0, 2 contribute to the real terms. The change in concavity does not affect the fact that $h_0 < h_1 < h_2 < h_3$, and $h_0 + h_1 < h_2 + h_3 / h_0 + h_2 < h_1 + h_3$.

As shown in Figure 11, to the left of the turning point, the imaginary region is made up from magnitudes of $h_1 + h_3 - (h_0 + h_2) > 0$. Then, we compare the positive-imaginary difference: $h_2 + h_3 - (h_0 + h_1) - (h_1 + h_3 - (h_0 + h_2)) = 2(h_2 - h_1) > 0$.

Similarly, to the right of the turning point, the positive region is made up from vertical lines of the magnitude $h_0 + h_1 - (h_2 + h_3) > 0$, while the real region is made up from $h_0 + h_2 - (h_1 + h_3) > 0$. Since $h_0 > h_1 > h_2 > h_3$ after TP, we have, for each index group real and positivity difference: $h_0 + h_2 - (h_1 + h_3) - (h_0 + h_1 - (h_2 + h_3)) = 2(h2 - h1) < 0$. These are also the same as the Type C graph.

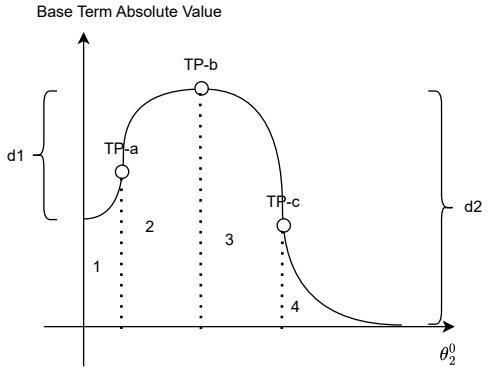

Figure 13: Type D graph characteristics. Depth d_1 is larger in magnitude compared to d_2. Region 3 + Region 4 > Region 1 + Region 2.

6.5 Type C/D Graph Characteristics

Figures 12 and 13 summarize the characteristics of the Type C/D graphs. See proofs in Appendix Section D. The characteristics will be helpful for our analysis for both the single term and the cross term sums.

6.6 "Imaginary Overflow" across Types B/C/D

As we assume the perfect positivity balance, the positivity graph can serve as the "groundtruth" shape required for balance. In other words, if the realness graph is always the same as the positivity graph, the Term-1-related components evaluate to zero when summed together. However, based on our earlier Types B/C/D graphs and the following reasons, the realness balance is impossible, and thus the zero existence within the Term-1-related components is contradictory.

Let the positive term-1-related components summed across all θ_2^0 for fixed n and $k = \theta_1^{t-4}$ be $P_{n,k}$, the negative components be $N_{n,k}$, the real components be $R_{n,k}$, and the imaginary components be $I_{n,k}$. Based on Eqn. 5.9 and the positivity balance, we have $\sum_{n,k} P_{n,k} + \sum_{n,k} N_{n,k} = 0 \Rightarrow |\sum_{n,k} P_{n,k}| = |\sum_{n,k} N_{n,k}|$.

We now analyse the relationship between $|\sum_{n,k} R_{n,k}|$ and $|\sum_{n,k} I_{n,k}|$ with respect to $|\sum_{n,k} P_{n,k}|$ and $|\sum_{n,k} N_{n,k}|$. In Type C/D graphs, due to the location of turning points, we have to pair the positive component with the real component, and the negative component with the imaginary component during the comparison. Let the magnitude $2|h_2 - h_1|$ (i.e., the imaginary-negative/real-positive magnitude difference) in the absolute Type C/D graph respectively be summed as D_{left} and D_{right} for index groups respectively before and after the peak turning points. Recall Figures 12 and 13, we have the depth d_1 before the turning point smaller than the depth d_2. Therefore, we have $D_{\text{left}} < D_{\text{right}}$. For the special Type B graph, $D_{\text{left}} = 0$. For the Type C/D graphs, suppose we always add D_{right} to both the imaginary and real area, the real area will match the positive area on the right side of the turning point exactly, but the imaginary area will overflow compared to the negative area, across all indices of n and $\theta_1^{t-4} = k$, that is $|\sum_{n,k} N_{n,k}| = |\sum_{n,k} I_{n,k} + D_{\text{left},n,k}| < |\sum_{n,k} I_{n,k} + D_{\text{right},n,k}|$. For

the Type B graph, the real region will match the positive region. Therefore, overall, we will have:

$$\begin{aligned}|\sum_{n,k} R_{n,k}| - |\sum_{n,k} I_{n,k}| &= (|\sum_{n,k} R_{n,k}| + D_{\text{right},n,k}) - (|\sum_{n,k} I_{n,k}| + D_{\text{right},n,k}) \\ &= |\sum_{n,k} P_{n,k}| - (|\sum_{n,k} I_{n,k}| + D_{\text{right},n,k}) \\ &< |\sum_{n,k} P_{n,k}| - |\sum_{n,k} N_{n,k}| \\ &= |\sum_{n,k} P_{n,k}| - (|\sum_{n,k} I_{n,k}| + D_{\text{left},n,k}).\end{aligned} \tag{6.2}$$

Therefore, in Type C/D, with respect to the positivity groundtruth balance, the realness balance is tipped to the imaginary side. Therefore, the zero within the Term-1 related components is impossible under the assumption of exact groupings.

6.7 Non-Exact Index Groupings

Previously, we assume that the turning point of the original absolute graph happens exactly at the last index 3, or the regions before the turning point **end** exactly at index 3, within the Term 1 scope. To complete all cases, we analyse what happens when the turning point in the positivity graph happens at the alternative positions, or indices 0, 1 and 2.

Case 1: Turning point of the positivity graph happens at indices 0 or 1: as illustrated in Figure 8, this case is impossible as the indices 0 or 1 contribute to the positive region after the turning point. Setting the turning point of the positivity graph at the indices 0 or 1 means forcing these positive values into the negative region before the turning point, which is contradictory to the graph set-up.

Case 2: Turning point of the positivity graph happens at index 2. This case is impossible as well since it requires h_2, which contributes to the negative region before the turning point, to be larger than $h_0 + h_1$ that contributes to the positive region after the turning point. In other words, we need to fulfill $h_2 > h_0 + h_1$. Due to the graph smoothness, the infinitely small horizontal gaps $\epsilon \to 0$ between h_0, h_1 and h_2 and their vertical magnitudes much larger than ϵ (e.g., $h_2 > \epsilon$), we have $h_0 \approx h_1 \approx h_2 \to h_0 + h_1 \approx 2h_2 > h_2$.

For the realness graph, turning points at indices 0, 2 are impossible because they contribute to the real region, while the region including the turning point is imaginary. The turning point at index 1 is also impossible due to the similar case 2 reasoning.

Overall, the grouping has to be exact for both the positivity and realness graphs.

7 Term 1 and 2 Overall Imbalance

Next, we focus on Term 2 analysis to cover the cross-term zero impossibility.

7.1 Graph Set-up.

We still refer to the following expression as the "Base Component":

$$\frac{(0.5)^{\theta_1^{t-4}}(0.5)^{\theta_2^0}}{\theta_1^{t-4}!\theta_2^0!} n^{-2}(\ln n)^{\theta_1^{t-4}+\theta_2^0} = \left[\frac{(0.5)^k}{k!} n^{-2}(\ln n)^k\right] \cdot \frac{(0.5\ln n)^x}{x!}, \tag{7.1}$$

where $x = \theta_2^0$ and let $k = \theta_1^{t-4}$. To recap, we assume RealDiff - ImagDiff$\cdot i = 0$. We fix n and θ_1^{t-4} to any general valid value.

Figures 14, 15 and 16 illustrate the B, C, D graph types for the Term 2 respectively.

To recap, each index type $\theta_2^0 \% 4$ contributes to the (RealDiff - ImagDiff$\cdot i$)$_{\text{Term 1}}$ in the following manner (See Eqn 5.10):

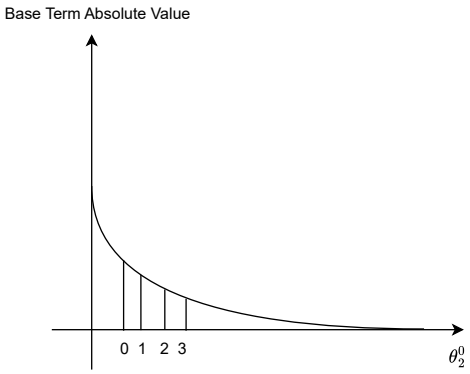

Figure 14: Type B absolute graph for Term 2.

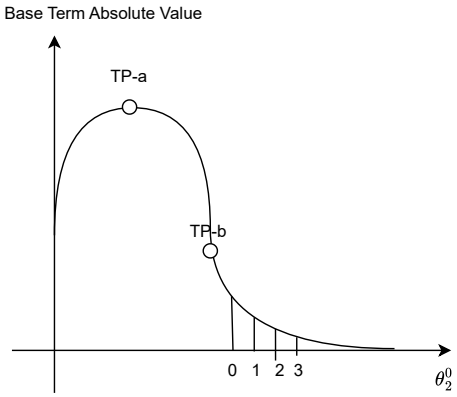

Figure 15: Type C absolute graph for Term 2.

1. Positive component: Indices 0, 3
2. Negative component: Indices 1, 2
3. Real Component: Indices 1, 3
4. Imaginary Component: Indices 0, 2

7.2 Type B Graph

We first evaluate the Type B absolute graph, which can be converted to the Figure 17 positivity graph and the Figure 18 realness graph. In the positivity graph, all values are, again, positive. In the realness graph, all values are imaginary. Compared to the Term 1 Type B realness graph, both the realness graph regions are made up of magnitudes of $|h_0 + h_2 - (h_1 + h_3)|$ from the original absolute Type b graph, and are the same in size.

7.3 Type C Graph

We next evaluate the type C absolute graph in Figure 4, which can be converted to the Figure 19 positivity graph and the Figure 20 realness graph.

In the positivity graph, all values to the left of the peak turning point is negative, and then becomes positive. To recap, indices 0 and 3 contribute to the positive component. In the realness graph, all

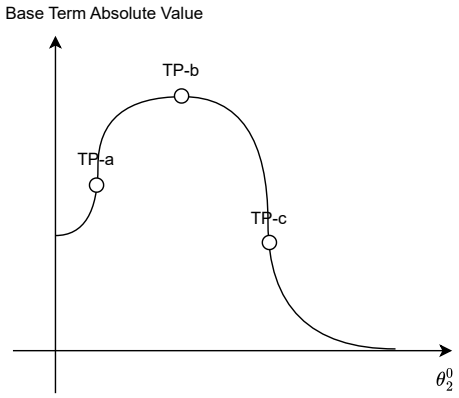

Figure 16: Type D absolute graph for Term 2.

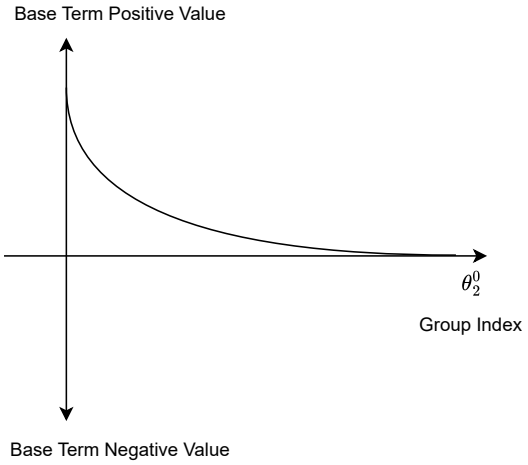

Figure 17: Type B Term 2 positivity graph.

values are real to the left of the peak turning point, and becomes imaginary to the right of the turning point. To recap, indices 0 and 2 contribute to the imaginary component.

Comparing the Term 2 imaginary area with the Term 1 imaginary area, we have the Term 2 imaginary area being larger than that of the Term 1, because both the area are made up with magnitudes of $|h_0 + h_2 - (h_1 + h_3)|$ of the same original absolute Type C graph, and the sum of the Region 2 and 3 after the turning point is larger than the Region 1 before the turning point (See Section 6.5. Recall that the Term 2 imaginary area takes place after the peak turning point, and the Term 1 imaginary area takes place before the turning point). Meanwhile, the Term 2 real area is smaller than the Term 1 real area due to the same reason.

7.4 Type D Graph

We next evaluate the type D absolute graph in Figure 5, which can be converted to the Figure 21 positivity graph and the Figure 22 realness graph.

In the positivity graph, all values to the left of the inflection turning point TP-a are positive, and then becomes negative until the left of the peak turning point TP-b, before becoming positive after the

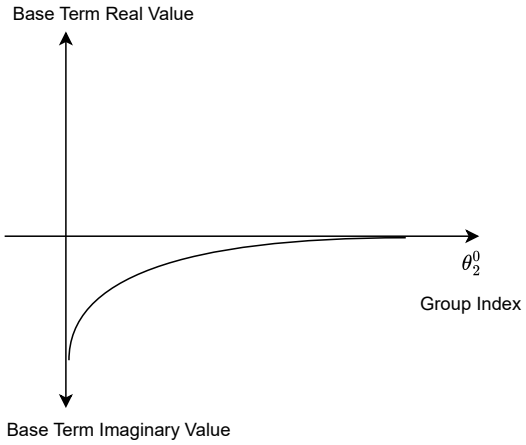

Figure 18: Type B Term 2 realness graph.

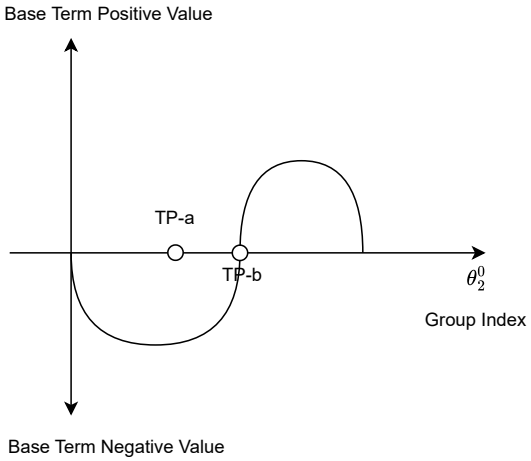

Figure 19: Type C Term 2 positivity graph.

last inflection turning point TP-c. To recap, indices 0 and 3 contribute to the positive component. In the realness graph, all values are real to the left of the inflection point TP-b, and becomes imaginary to the right of TP-b.

Comparing the Term 2 imaginary area with the Term 1 imaginary area, we also have the Term 2 imaginary area being larger than that of the Term 1, because both the area are made up with magnitudes of $|h_0 + h_2 - (h_1 + h_3)|$ of the same original absolute Type C graph, and the sum of the Region 3 and 4 after the turning point is larger than the Region 1 and 2 before (See Section 6.5). Meanwhile, the Term 2 real area is also smaller than the Term 1 real area due to the same reason.

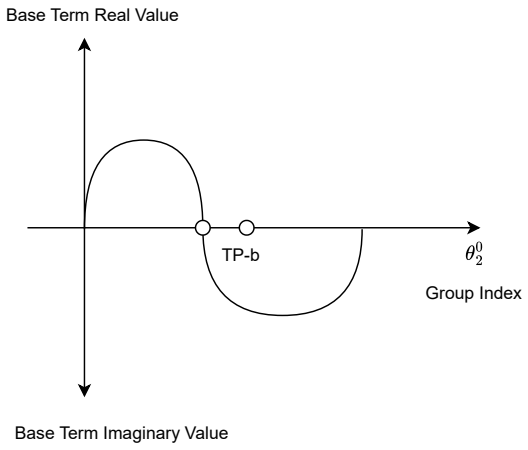

Figure 20: Type C Term 2 realness graph.

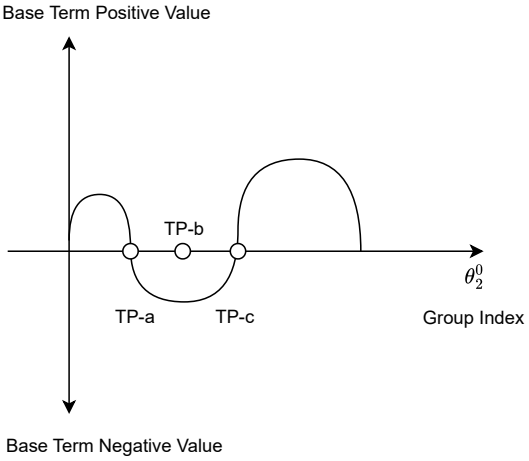

Figure 21: Type D Term 2 positivity graph.

7.5 The Contradiction Associated With Term 1+2

Assuming the cross-term realness balance, we have:

$$\begin{aligned}
&\sum_{n,k} R_{\text{Term 1},n,k} \cos(n \ln n) + \sum_{n,k} I_{\text{Term 1},n,k} \cos(n \ln n) + \\
&\sum_{n,k} R_{\text{Term 2},n,k} \sin(n \ln n) + \sum_{n,k} I_{\text{Term 2},n,k} \sin(n \ln n) = 0 \\
&A \sum_{n,k} R_{\text{Term 1},n,k} + A \sum_{n,k} I_{\text{Term 1},n,k} + B \sum_{n,k} R_{\text{Term 2},n,k} + B \sum_{n,k} I_{\text{Term 2},n,k} = 0 \qquad (7.2) \\
&\underbrace{A \sum_{n,k} R_{\text{Term 1},n,k} + B \sum_{n,k} R_{\text{Term 2},n,k}}_{=0} + \underbrace{A \sum_{n,k} I_{\text{Term 1},n,k} + B \sum_{n,k} I_{\text{Term 2},n,k}}_{=0} = 0,
\end{aligned}$$

where A and B are the constant weights caused by the different $\cos(n \ln n)$ and $\sin(n \ln n)$ factors for Term 1 and 2 respectively.

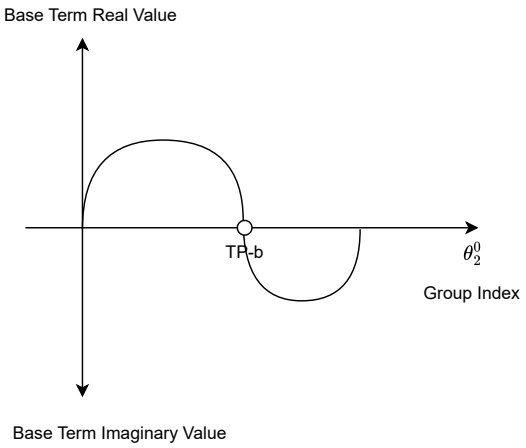

Figure 22: Type D Term 2 realness graph.

As we have earlier deduced, we have the Term 2 imaginary area always being larger than or equal to that of the Term 1 across all graph types B/C/D, for all specific indices of n and $k = \theta_1^{t-4}$. That is: $\sum_{n,k} I_{\text{Term 2},n,k} > \sum_{n,k} I_{\text{Term 1},n,k}$. Therefore, for $A \sum_{n,k} I_{\text{Term 1},n,k} + B \sum_{n,k} I_{\text{Term 2},n,k} = 0$, we need $B < A$. Also, we have the Term 2 real area always being smaller than the Term 1 real area. That is: $\sum_{n,k} R_{\text{Term 2},n,k} < \sum_{n,k} R_{\text{Term 1},n,k}$. Therefore, for $A \sum_{n,k} R_{\text{Term 1},n,k} + B \sum_{n,k} R_{\text{Term 2},n,k} = 0$, we need $A < B$. Therefore, we derive a contradiction with both $B < A$ and $A > B$.

7.6 Non-Exact Index Groupings

Our Term 2 analysis mainly focuses on comparing the Type C/D Term 1 and 2 imaginary and real magnitudes, based on region area comparison. For this comparison, the conclusion holds regardless of the locations of the shared absolute magnitude graph turning points.

8 Sanity Checks and Remarks

Alongisde the fact that the non-trivial zeroes do not exist between $y = -2$ and $y = 2$ in the original zeta function complex plane, we cover the entire critical strip.

Since the RealDiff - ImagDiff$\cdot i = 0$ is a necessary condition for the existence of non-trivial zeros, the fact that RealDiff - ImagDiff$\cdot i \neq 0$ proves the non-existence of the non-trivial zeros.

Our proof also shows that it is possible to have 0 on the critical line itself, since RealDiff - ImagDiff$\cdot i = 0$ when the final horizontal shift $\Delta_{t,1} = 0$.

9 Conclusion

To conclude, we first derive the analytical continuation of the Riemann's Zeta function via a chained disk formulation. We then derive the real and imaginary value difference, called RealDiff - ImagDiff$\cdot i$, between the off-line symmetric point values, which can never be zero by simplistic logical deductions. Since the difference being zero is a necessary condition for the off-line zero existence, we conclude that the Riemann's Hypothesis is true unconditionally.

A Derivation Details for the Recursive Chained Disk Representation

First, we rewrite the terms of the Dirichlet series for the Riemann zeta function, valid in the region of absolute convergence. Let $s = x + iy$. The general term is expressed using the complex exponential:

$$n^{-s} = e^{-s \ln n} = e^{-(x+iy) \ln n} \tag{A.1}$$

Next, we compute the partial derivative with respect to the real part, x:

$$\frac{\partial}{\partial x} \left(e^{-(x+iy) \ln n} \right) = (-\ln n) e^{-(x+iy) \ln n} = (-\ln n) n^{-s} \tag{A.2}$$

Applying this differentiation operator θ_1^0 times yields:

$$\frac{\partial^{\theta_1^0}}{\partial x^{\theta_1^0}} (n^{-s}) = (-\ln n)^{\theta_1^0} n^{-s} = (-1)^{\theta_1^0} (\ln n)^{\theta_1^0} n^{-s} \tag{A.3}$$

Similarly, we compute the partial derivative with respect to the imaginary part, y:

$$\frac{\partial}{\partial y} \left(e^{-(x+iy) \ln n} \right) = (-i \ln n) e^{-(x+iy) \ln n} = (-i \ln n) n^{-s} \tag{A.4}$$

Applying this differentiation operator θ_2^0 times yields:

$$\frac{\partial^{\theta_2^0}}{\partial y^{\theta_2^0}} (n^{-s}) = (-i \ln n)^{\theta_2^0} n^{-s} = (-i)^{\theta_2^0} (\ln n)^{\theta_2^0} n^{-s} \tag{A.5}$$

Combining these results, the mixed partial derivative of order (θ_1^0, θ_2^0) for a single term is:

$$\partial^{(\theta_1^0, \theta_2^0)} (n^{-s}) = (-1)^{\theta_1^0} (-i)^{\theta_2^0} (\ln n)^{\theta_1^0 + \theta_2^0} n^{-s} \tag{A.6}$$

Summing over all $n \geq 1$, the full mixed partial derivative of the series evaluates to:

$$\partial^{(\theta_1^0, \theta_2^0)} \zeta(s) = \sum_{n=1}^{\infty} (-1)^{\theta_1^0} (-i)^{\theta_2^0} (\ln n)^{\theta_1^0 + \theta_2^0} n^{-s} \tag{A.7}$$

Evaluating this derivative at the base point $a_0 = 2 + 2i$, we substitute $s = 2 + 2i$:

$$n^{-(2+2i)} = n^{-2} n^{-2i} = n^{-2} e^{-i(2 \ln n)} \tag{A.8}$$

Substituting this back into the summation yields the expression:

$$\partial^{(\theta_1^0, \theta_2^0)} \zeta(a_0) = (-1)^{\theta_1^0} (-i)^{\theta_2^0} \sum_{n=1}^{\infty} n^{-2} (\ln n)^{\theta_1^0 + \theta_2^0} e^{-i2 \ln n} \tag{A.9}$$

To extract the explicit real and imaginary components, we convert the $(-i)^{\theta_2^0}$ multiplier into its polar exponential form, $-i = e^{-i\frac{\pi}{2}}$, which provides:

$$(-i)^{\theta_2^0} = e^{-i\frac{\pi}{2}\theta_2^0} \tag{A.10}$$

Merging the complex exponentials, we obtain:

$$e^{-i\frac{\pi}{2}\theta_2^0} e^{-i2 \ln n} = e^{-i\left(\frac{\pi}{2}\theta_2^0 + 2 \ln n\right)} \tag{A.11}$$

Applying Euler's formula, $e^{-ix} = \cos x - i \sin x$, separates the term into its real and imaginary coordinates:

$$e^{-i\left(\frac{\pi}{2}\theta_2^0 + 2 \ln n\right)} = \cos\left(\frac{\pi}{2}\theta_2^0 + 2 \ln n\right) - i \sin\left(\frac{\pi}{2}\theta_2^0 + 2 \ln n\right) \tag{A.12}$$

Isolating the purely real part produces:

$$\Re\left[\partial^{(\theta_1^0,\theta_2^0)}\zeta(a_0)\right] = (-1)^{\theta_1^0}\sum_{n=1}^{\infty} n^{-2}(\ln n)^{\theta_1^0+\theta_2^0}\cos\left(\frac{\pi}{2}\theta_2^0 + 2\ln n\right) \tag{A.13}$$

Isolating the purely imaginary part produces Equation:

$$\Im\left[\partial^{(\theta_1^0,\theta_2^0)}\zeta(a_0)\right] = (-1)^{\theta_1^0}\sum_{n=1}^{\infty} n^{-2}(\ln n)^{\theta_1^0+\theta_2^0}\left(-\sin\left(\frac{\pi}{2}\theta_2^0 + 2\ln n\right)\right) \tag{A.14}$$

B Symmetry of Non-Trivial Zeros Across the Critical Line

We first explain why that RealDiff - ImagDiff$\cdot i = 0$ is a necessary condition for the existence of off-line non-tirivial zeros.

Let $p_2 = \sigma + it$ be an assumed non-trivial zero of the Riemann zeta function lying off the critical line, such that $\sigma \neq 0.5$ and $0 < \sigma < 1$. The point horizontally symmetric to p_2 across the critical line $\Re(s) = 0.5$ is geometrically defined as $p_1 = 1 - \sigma + it$.

To demonstrate that $\zeta(p_1) = 0$ strictly follows from $\zeta(p_2) = 0$, we rely on two fundamental analytic properties of the Riemann zeta function: the Schwarz reflection principle and the Riemann functional equation.

First, because the Dirichlet series coefficients of $\zeta(s)$ are real, the Schwarz reflection principle establishes that for any complex number s:

$$\zeta(\overline{s}) = \overline{\zeta(s)}$$

Given the assumption that $\zeta(p_2) = 0$, it immediately follows that its complex conjugate is also a zero:

$$\zeta(\sigma - it) = 0$$

Second, the analytic continuation of the zeta function to the entire complex plane satisfies the Riemann functional equation:

$$\zeta(s) = 2^s\pi^{s-1}\sin\left(\frac{\pi s}{2}\right)\Gamma(1-s)\zeta(1-s)$$

Within the critical strip $0 < \Re(s) < 1$, the product of the pre-factors $2^s\pi^{s-1}\sin\left(\frac{\pi s}{2}\right)\Gamma(1-s)$ is strictly non-zero. Therefore, a zero can only occur if the corresponding evaluated term $\zeta(1-s)$ is zero, meaning the roots of $\zeta(s)$ and $\zeta(1-s)$ must perfectly coincide in this region.

Applying this exact functional symmetry to the conjugate zero $\overline{p_2} = \sigma - it$, we map the zero to its reflection:

$$\zeta(1 - (\sigma - it)) = \zeta(1 - \sigma + it) = 0$$

Recognizing that $1 - \sigma + it$ is precisely the coordinates of the horizontally symmetric point p_1, we conclude:

$$\zeta(p_1) = 0$$

Thus, if an off-line zero p_2 evaluates to zero, its horizontal reflection across the critical line, p_1, is analytically guaranteed to also evaluate to zero. This necessitates that their calculated difference equals strictly zero, forcing the system into the exact geometric balance evaluated by the RealDiff and ImagDiff equations.

C Vertical Symmetry of Zeros Across the Real Axis

Next, we prove why covering only the upper part of the critical strip simultaneously covers the analysis for the lower part of the critical strip.

Building upon the horizontal symmetry established across the critical line, we must also account for the vertical symmetry of the non-trivial zeros across the real axis (where $\Im(s) = 0$).

The Dirichlet series for the Riemann zeta function, $\zeta(s) = \sum_{n=1}^{\infty} n^{-s}$, possesses strictly real coefficients. Consequently, the analytic continuation of $\zeta(s)$ maps real inputs to real outputs. By the Schwarz reflection principle, any analytic function that is real-valued on the real axis satisfies the conjugate equality for all complex numbers s:

$$\zeta(\overline{s}) = \overline{\zeta(s)}$$

Let $p_2 = \sigma + it$ be an assumed off-line zero such that $\zeta(p_2) = 0$. Applying the reflection principle directly to this point yields:

$$\zeta(\overline{p_2}) = \zeta(\sigma - it) = \overline{\zeta(\sigma + it)} = \overline{0} = 0$$

Thus, the vertically symmetric point $\overline{p_2}$ must also be a zero.

Furthermore, we previously established via the Riemann functional equation that if p_2 is a zero, its horizontal reflection across the critical line, $p_1 = 1 - \sigma + it$, must concurrently be a zero (i.e., $\zeta(p_1) = 0$). Applying the Schwarz reflection principle to p_1 dictates:

$$\zeta(\overline{p_1}) = \zeta(1 - \sigma - it) = \overline{\zeta(1 - \sigma + it)} = \overline{0} = 0$$

Therefore, if any single off-line zero $p_2 = \sigma + it$ is assumed to exist, it analytically necessitates the existence of a symmetric quartet of zeros in the critical strip:

$$(p_2, \overline{p_2}, p_1, \overline{p_1}) = (\sigma + it, \sigma - it, 1 - \sigma + it, 1 - \sigma - it)$$

If either p_1 or p_2 evaluates to zero, their corresponding vertically symmetric points, reflected across the real axis, are analytically guaranteed to also evaluate to zero.

D Graph C/D Characteristics

First, for both graph C and D, it is obvious that $d_1 < d_2$, since the simplified base component expression $f(x) = \frac{(0.5 \ln n)^x}{x!}$ starts from 1 when $x = 0$ and tends towards the 0 asymptote at the end. Next, we provide the proof for that the region before the turning point is smaller than the region after the turning point.

Setup and the Asymmetry. Let $f(x) = \frac{\lambda^x}{\Gamma(x+1)}$ where $\lambda = 0.5 \ln n$ for integers $n \geq 3$. Let x_m be the unique mode (peak) where $f'(x_m) = 0$.

We define the log-space function $g(x) = \ln f(x) = x \ln \lambda - \ln \Gamma(x+1)$. The shape of the distribution is governed by the derivatives of $g(x)$:

$$\begin{aligned} g'(x) &= \ln \lambda - \psi(x + 1) \\ g''(x) &= -\psi_1(x + 1) \\ g'''(x) &= -\psi_2(x + 1) \end{aligned}$$

where ψ, ψ_1, and ψ_2 are the digamma, trigamma, and tetragamma functions, respectively.

A fundamental property of the tetragamma function is that $\psi_2(z) < 0$ for all real $z > 0$. Therefore, we have an absolute mathematical rule: $g'''(x) > 0$ strictly across the entire domain $x > 0$. This implies that $g''(x)$ is a strictly increasing function (it becomes less negative as x increases), and consequently, $g'(x)$ is a strictly convex function.

Step 1: Formalizing the Gradient Imbalance. We compare the magnitude of the log-gradient at a horizontal distance t to the left of the peak against the gradient at the same distance t to the right of the peak, for any $0 < t \leq x_m$.

Using the Fundamental Theorem of Calculus, the log-gradients moving away from the peak are:

$$g'(x_m + t) = \int_0^t g''(x_m + u)\, du \quad \text{(falling right side)}$$
$$g'(x_m - t) = -\int_0^t g''(x_m - u)\, du \quad \text{(rising left side)}$$

Because $g''(x)$ is strictly increasing, the negative curvature on the left is always more severe than the negative curvature on the right. For any $u > 0$:

$$g''(x_m - u) < g''(x_m + u) < 0.$$

Taking the absolute values (the magnitude of the curvature):

$$|g''(x_m - u)| > |g''(x_m + u)|$$

Integrating these magnitudes over the distance t proves the exact gradient imbalance:

$$|g'(x_m - t)| > |g'(x_m + t)|.$$

This demonstrates that moving away from the peak, the left side falls off with a strictly steeper log-gradient than the right side.

Step 2: Translating Gradient to Height. Because the log-gradient magnitude dictates the rate of decay, the steeper drop on the left means the function value is strictly smaller than the mirrored counterpart on the right.

We prove this by integrating the log-gradients. Let $D(t)$ be the difference in log-heights:

$$\begin{aligned} D(t) &= g(x_m + t) - g(x_m - t) \\ &= \int_0^t \left[g'(x_m + u) - (-g'(x_m - u))\right] du \\ &= \int_0^t \left[g'(x_m + u) + g'(x_m - u)\right] du. \end{aligned}$$

Because $g'(x)$ is strictly convex, the Jensen's Inequality guarantees that the midpoint of any secant line sits above the curve. For any $u > 0$:

$$g'(x_m + u) + g'(x_m - u) > 2g'(x_m) = 0.$$

Since the integrand is strictly positive, the integral $D(t)$ is strictly positive for all $t > 0$:

$$g(x_m + t) > g(x_m - t) \implies f(x_m + t) > f(x_m - t)$$

Thus, for every point between 0 and the peak, its mirrored counterpart on the right side is strictly taller. Therefore, the right-tail region after the peak is larger than the left-tail region before the peak.